

# WARSAW UNIVERSITY OF TECHNOLOGY

Faculty of Power and Aeronautical Engineering

*“Czapla”*



## Design report of a cargo model aircraft

SAE Aero Design East 2023

WUT Regular

Team number 035

Team Members: Michał Włodarczyk; Antoni Szczurko; Bartosz Ziężo, Maciej Kupras;

Monika Mederska; Julia Lesiuk

## APPENDIX A - STATEMENT OF COMPLIANCE

---

### Certification of Qualification

Team Name WUT REGULAR Team Number 035  
School WARSAW UNIVERSITY OF TECHNOLOGY  
Faculty Advisor TOMASZ GOETZENDORF - GRABOWSKI, D.Sc., Ph.D., ENG  
Faculty Advisor's Email tgrab@meil.pw.edu.pl

### Statement of Compliance

As faculty Adviser:

✓ (Initial) I certify that the registered team members are enrolled in collegiate courses.

✓ (Initial) I certify that this team has designed and constructed the radio-controlled aircraft in the past nine (9) months with the intention to use this aircraft in the 2023 SAE Aero Design competition, without direct assistance from professional engineers, R/C model experts, and/or related professionals.

✓ (Initial) I certify that this year's Design Report has original content written by members of this year's team.

✓ (Initial) I certify that all reused content have been properly referenced and is in compliance with the University's plagiarism and reuse policies.

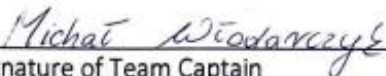
✓ (Initial) I certify that the team has used the Aero Design inspection checklist to inspect their aircraft before arrival at Technical Inspection and that the team will present this completed checklist, signed by the Faculty Advisor or Team Captain, to the inspectors before Technical Inspection begins.



Signature of Faculty Advisor

26.01.2023

Date



Signature of Team Captain

26.01.2023

Date

Note: A copy of this statement needs to be included in your Design Report as page 2 (Reference Section 4.3)

## Table of Contents

Table of Figures.....	- 4 -
Table of Tables .....	- 4 -
Table of Symbols and Acronymes.....	- 4 -
Table of References.....	- 4 -
1. Executive Summary .....	- 5 -
1.1 Introduction and goals .....	- 5 -
1.2 Discriminators.....	- 5 -
2. Project overview .....	- 6 -
2.1 Schedule and plans .....	- 6 -
2.2 Resources and costs .....	- 7 -
2.3 Risk analysis, validation.....	- 8 -
3. Design Layout and Trades .....	- 9 -
3.1 Scoring analysis and strategy.....	- 9 -
3.2 Design process.....	- 9 -
3.2.1 Initial design and vehicle configuration selection .....	- 9 -
3.2.2 Wing design.....	- 11 -
3.2.3 Airfoil selection.....	- 12 -
3.2.4 Tail design .....	- 13 -
3.2.5 Fuselage, cargo bay and landing gear .....	- 13 -
3.2.6 Mass and balance.....	- 14 -
3.2.7 Propulsion selection.....	- 15 -
3.2.8 Vehicle sizing and servo selection .....	- 16 -
3.2.9 Structural analysis, load and material selection .....	- 16 -
3.2.10 Spar wall structure and testing.....	- 18 -
3.2.11 Wing static test .....	- 18 -
3.3 Final structure design .....	- 19 -
3.3.1 Assembly .....	- 19 -
3.3.2 Design features.....	- 19 -
4. Performance Analysis .....	- 21 -
4.1 General .....	- 21 -
4.2 Weather conditions.....	- 21 -
4.3 Take off and climb analysis .....	- 21 -
4.4 Stability and control .....	- 22 -
4.5 Turn Radius Analysis .....	- 24 -
4.6 Polar curve and landing distance .....	- 24 -
4.7 Payload prediction and lifting performance.....	- 25 -
5. Manufacturing .....	- 26 -
6. Conclusions .....	- 28 -
Appendices.....	- 28 -

## Table of Figures

Fig. 1	Discriminators	-5-	Fig. 18	Adapters for the tail boom segments (joined)	-20-
Fig. 2	Project schedule	-6-	Fig. 19	Take-off analysis	-21-
Fig. 3	Cost breakdown (own elaboration)	-7-	Fig. 20	Take-off analysis	-22-
Fig. 4	Scheme and assumptions for each stage of configuration selection	-10-	Fig. 21	Climb rate analysis	-22-
Fig. 5	Results of 1st stage of optimisation- expected FFS for different wingspan and AR	-10-	Fig. 22	Static margin vs. angle of attack	-23-
Fig. 6	Structure of a wing	-11-	Fig. 23	Pitching moment coefficient vs. angle of attack	-23-
Fig. 7	Lift and drag coefficients plotted against attack angle	-12-	Fig. 24	Dutch roll characteristics against the background of MIL-F8785C specification	-23-
Fig. 8	Final wing planform with airfoils	-12-	Fig. 25	Spiral mode time to double against the background of MIL-F8785C specification	-23-
Fig. 9	Comparison of different configurations of the aircraft	-13-	Fig. 26	Turn radius analysis	-24-
Fig. 10	Fuselage and its compnts	-14-	Fig. 27	Polar curve analysis	-24-
Fig. 11	Wind tunnel propulsion testing	-15-	Fig. 28	Landing analysis	-25-
Fig. 12	Propeller performance comparison (left), selected propeller thrust characteristics (right)	-15-	Fig. 29	In-house manufacturing of servo-ribs	-26-
Fig. 13	Flight envelope	-17-	Fig. 30	3D SLS printed element of center wing-electroc bay	-26-
Fig. 14	Bending moment	-18-	Fig. 31	3D SLS printed element of tail boom	-26-
Fig. 15	Exploded view	-19-	Fig. 32	D-box covers during vacuum gluing	-27-
Fig. 16	Wing and electronic bay	-19-	Fig. 33	Spare flange positioning device, acrylic retainer	-27-
Fig. 17	Tail boom exploded view with adapter	-20-	Fig. 34	D-box covers during gluing to the wing structure	-27-

## Table of Tables

Table 1.	– Mass of parts	-14-
Table 2.	– Hinge moments on control surfaces	-16-
Table 3.	– Weather conditions	-21-

## Table of Symbols and Acronyms

AR	– Aspect Ratio	M <sub>0</sub>	– Empty Weight
CAD	– Computer Aided Design	MTOW	– Maximum Take – Off Weight
CG	– Center of Gravity	Re <sub>MIN</sub>	– Reynolds number corresponding to stall speed
C <sub>L</sub>	– Lift coefficient	T <sub>NOM</sub>	– Nominal torque
C <sub>Lmax</sub>	– Maximal lift coefficient	TO	– Take – Off
CNC	– Computer Numerical Control	TR	– Taper ratio
FFS	– Final Flight Score	TR	– Taper Ratio
Fig.	– Figure	V <sub>c</sub>	– Cruise speed
FOS	– Factor of safety	V <sub>D</sub>	– Diving speed
FS	– Flight Score	WS	– Wingspan Score
L/D	– Lift to Drag ratio	WUT	– Warsaw University of Technology
MAC	– Mean Aerodynamic Chord		

## Table of References

[1]	– Fixed-wing unmanned aerial vehicle wing design (Engineering Thesis); Piotr Pacuszk	-11-
[2]	– Feasibility Study Of Lightweight High-strength Hollow Core Balsa; Kevin O’Neil	-18-
[3]	– Study of the spar wall structure of the “Regular” class UAV for the SAE Aero Design 2022 competition	-16-

## 1. Executive Summary

---

### 1.1 Introduction and goals

WUT SAE AeroDesign Collegiate Club hereby presents the 2023 Regular class aircraft, "Czapla". The main goal of the SAE Aero Design 2023 competition is to design an aircraft with a short take-off distance, as well as the greatest possible wingspan and payload capability. This year's strategy is based on maximizing WS bonus points, therefore we assumed monoplane wing configuration with 216 in wingspan. The main goal was to maintain a simple structure, time – saving manufacturing and fast cargo unloading. By optimizing aerodynamics and structure design, the plane is expect to lift 16.53 lbs payload.

### 1.2 Discriminators

Our airframe has a conventional configuration with wing divided into five sections and single half split tail boom to meet single part dimension requirement. High aspect ratio reduces induced drag. Extended stability analysis resulted in a polyhedral wing that significantly improves spiral stability for a more enjoyable flight experience. Cargo bay is located in the fuselage below center wing. The aircraft has been designed for ease of operation in the field and for ease of maintenance.

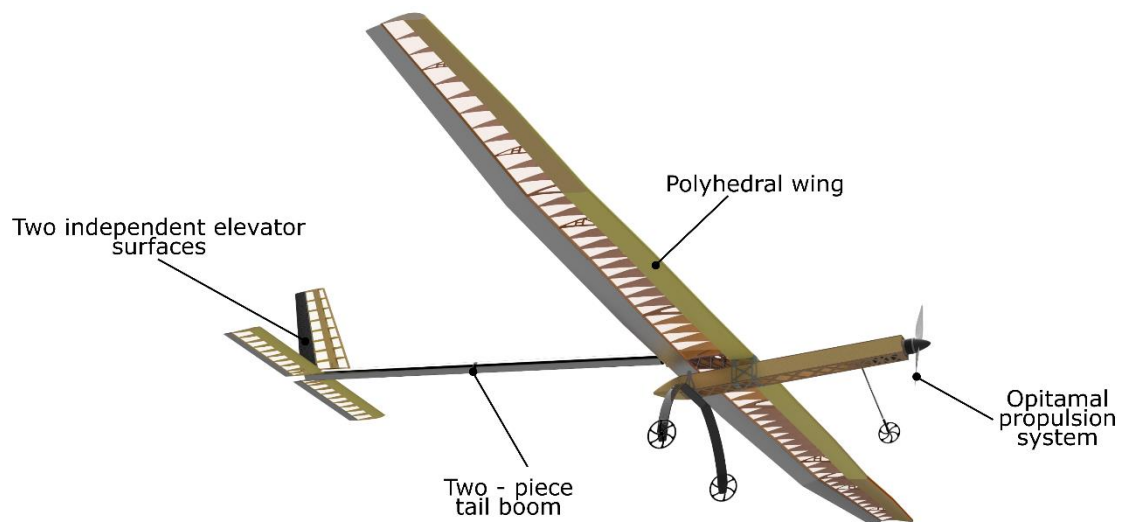


Fig. 1. Discriminators

## 2. Project overview

In this year's edition of the competition we decided to participate in two classes – Regular and Micro. Each class has its coordinator and vice – coordinator who are responsible for designing and manufacturing the aircraft. Using the experience from previous editions, we significantly increased work efficiency and management techniques in the SAE AeroDesign Warsaw Student Association. Due to the timing of the publication of the regulations, we had to design and build the aircraft within 6 months. We set ourselves the ambitious task of building the largest aircraft in the history of our association. We based our communication on MS Teams and OneDrive. It improved the connection between team members, especially designers and CNC operators. Moreover, we used ClickUp app to track schedule and work progress. During design process we used XFLR5 and AVL for aerodynamics and stability design, XoptFoil for airfoil design, MATLAB and MS Excel for optimization and Siemens NX for structure design. Most of the aircraft parts were manufactured in our workshop at the University. We have used wind tunnel at our faculty for propulsion selection and tests.

### 2.1 Schedule and plans

We started working on strategy analysis as soon as new rules were released. During the first three weeks, we conducted initial optimization, which led to a decision for the classic configuration with a maximum wingspan. By the end of September, we performed initial propulsion system test to gain data required for take – off and climb performance analysis and for the final configuration selection.

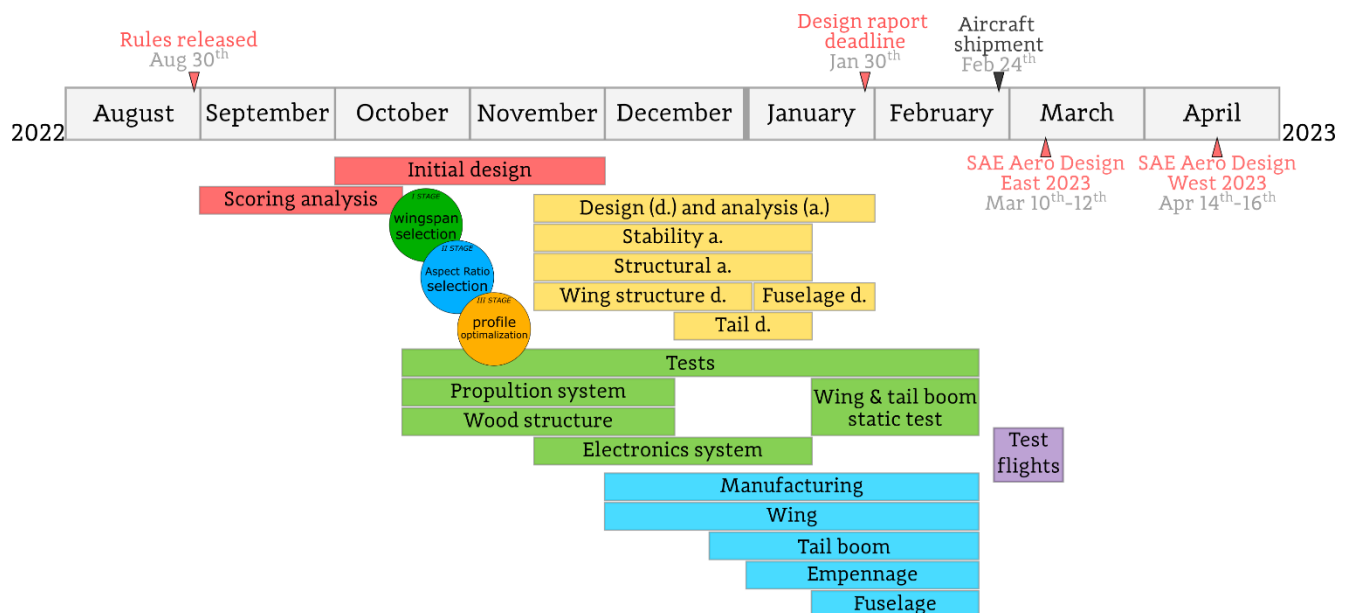


Fig. 2. Project schedule

Simultaneously, we carried out material strength measurement of wooden structures. We started manufacturing wing and tail boom in the last week of November. We divided the workshop work into individual subsections, and each was headed by a person responsible for a given aircraft component. This way of organization significantly improved the efficiency of the aircraft manufacturing. The team met once a week to track the progress in work done and divide new tasks. We planned to manufacture two complete planes. A more detailed schedule is presented in Fig. 2.

## 2.2 Resources and costs

Main challenge in this edition was to design and manufacture planes for the Regular and Micro class within six months. Thanks to the funding received from sponsors and institutions such as the University or the Ministry of Education and Science, we could afford to build an aircraft with 216 in span. Most of our aircraft is made of balsa, plywood and aviation aluminum alloy to obtain material restrictions. An important factor we had to consider this year was the availability of balsa wood in Europe. During previous years we selected each balsa' plank to find those which matched our specification. This year, we had to accept large variances between individual sheets, as we could not hand pick the ones we wanted. This limited us in terms of reducing the mass of the structure. The relatively large differences between strength related to density were considered during structure design process.

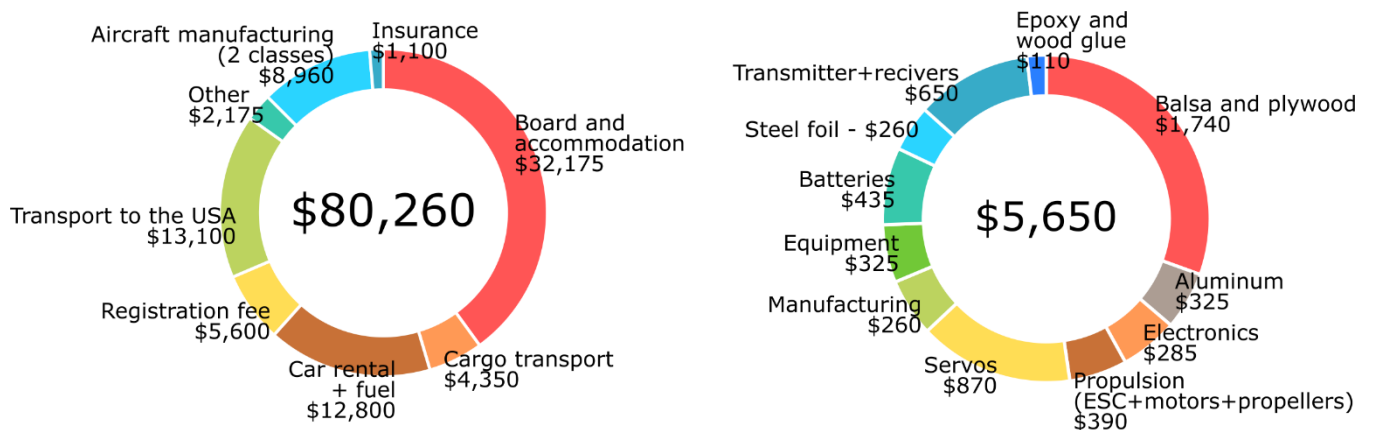


Fig. 3. Cost breakdown (own elaboration)

Moreover, to reduce costs and increase the time efficiency of production, we decided to make most of the elements ourselves. Only in exceptional cases requiring high accuracy and special equipment we outsourced machining to third party companies. As we planned to participate in SAE Aero Design East and West we carefully planned budget for aircraft manufacturing and travel knowing the rising cost of supplies and travel related costs.

## 2.3 Risk analysis, validation

Safety is critical in the design of the aircraft, especially due to the size of our plane. This required careful analysis of risks and potential issues in various areas. Firstly, we performed the analysis with the usage of safety factors on different components. To increase our understanding of balsa mechanical properties, we conducted several strength tests that gave us accurate data used in the design phase. As we decided to participate in both SAE Aero Design editions – East and West, we designed our plane for expected weather conditions in Texas in the middle of April, as the conditions will be more challenging than in Florida, with lower air density and stronger wind gusts, according to the climate data. We plan to perform static test of the wing and tail boom to verify structure reliability with 100% assumed load. We decided to build a training wing with a simple, robust and easy to repair structure for tests and for practice for our pilot. The reliability of high – quality electronic components were also tested under expected load. Moreover, we divided electronics into quick – to – replace modules to limit the maintenance time at the field, understanding risk of failure due to faulty component, weather conditions or human error. In case of serious problems, we have compatible replacement modules with components from different manufacturers. As testing will not eliminate the risk of electronics failure, we implemented parallelly working receivers, separate battery pack for receiver, servos and redundant control surfaces of ailerons and elevators. In case of accident we plan to manufacture two complete competition planes and also training wing for test and practise flights before competition. We plan first test flights in US. Before aircraft shippment we will perform wind tunnel test of wing to (section 3.2.3). To reduce risk of wing joints we performed FEM analisys of spar flanges joints to ensure safety of design.



### 3. Design Layout and Trades

---

#### 3.1 Scoring analysis and strategy

Analysis of the scoring rules showed us the crucial role of wingspan, payload and structure mass in determining the FFS. We started initial design with comparison of possible configurations. Firstly, we rejected tailless configuration, both delta and flying wing, due to the disproportionate time required to work on stability analysis and test flights, compared to potential profits. Biplane and triplane configurations were rejected due to low experience with such designs and expected low directional stability that can be very dangerous in windy conditions. Therefore, we decided to analyze scoring for classical monoplane configuration. Because of many possible aircrafts planform designs we decided to perform calculations comparing performance and expected FFS of monoplane with wingspan between 120 in and 216 in. We prepared program that estimated basic parameters such as aircraft parts mass basing on wingspan and wing surface; the batch data was based on ours designs from previous years. We estimated also fuselage and empennage drag, as well as landing gear parameters in order to increase the accuracy. An analysis of take – off and climb performance was performed on more than fifteen wing designs with different span and aspect ratios, and found that maximizing these parameters produced the best results. In the end, we decided to select a 216 in wingspan, and 3162 sq. in. surface. It results with: FS = 13.27, WS = 24.25 points, FFS = 63.05.

#### 3.2 Design process

##### 3.2.1 Initial design and vehicle configuration selection

Decision to design aircraft in classic monoplane configuration led us to divide the optimization process into three steps: wingspan selection, AR selection with fixed wingspan and profile optimization. Fig. 4 shows the scheme and main assumptions for each stage. The main objective of the initial analysis was to find the balance between wingspan (greater wingspan – higher empty) mass and payload lifted. For this reason, we developed a simulation of take – off and performance during the climb using MATLAB software. We compared multiple wingspan and aspect ratio configurations, with approximated structure mass. In XFLR5 software we analyzed aerodynamic performance.

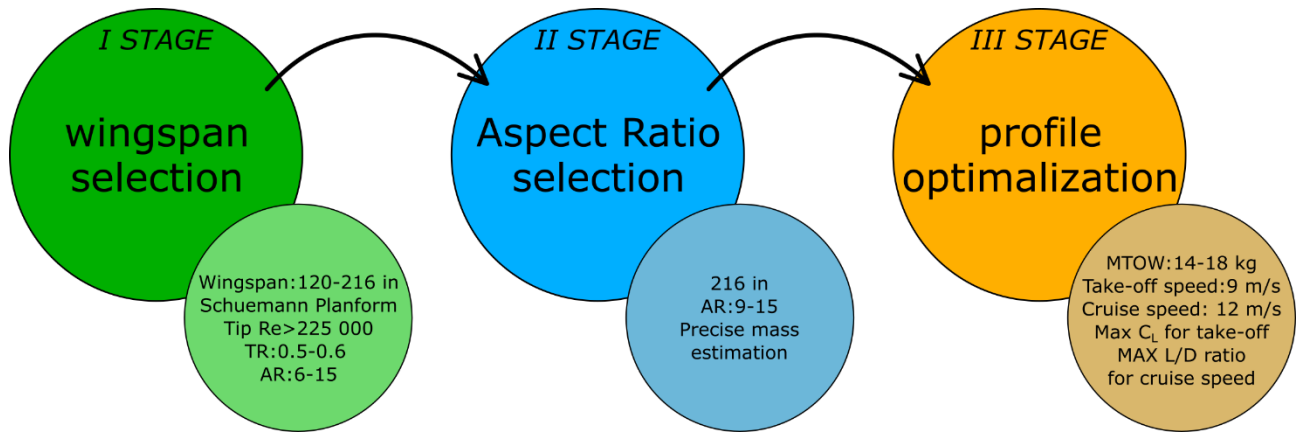


Fig. 4. Scheme and assumptions for each stage of configuration selection

For each wing we used LR315 airfoil developed in our association for regular class in 2019. Assumed limitations were: take – off distance, assumed 400 ft/min minimum climb rate (safety of flight) and cruise speed. The final output of these calculations was MTOW, payload and FS for each configuration. As a result, we decided to design the aircraft with a maximum wingspan. Fig. 5 plots expected FFS for considered AR and wingspan range.

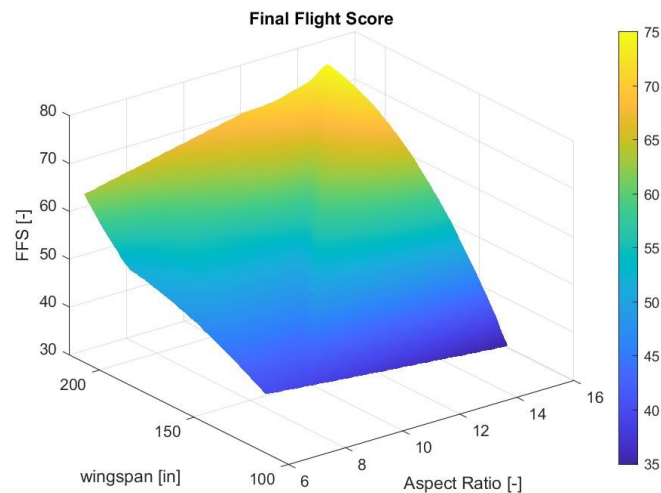


Fig. 5. Results of 1<sup>st</sup> stage of optimisation - expected FFS for different wingspan and AR

During the second stage of optimization, we decided to compare the wing's performance with 216 in wingspan and aspect ratio (AR) between 8 and 15, corresponding to surface of 40 ft<sup>2</sup> and 21,5 ft<sup>2</sup>. Based on analysis results, we could expect higher FS with higher AR, however it would result in lower Re number on the wingtip (smaller tip chord) and heavier structure. We used similar methodology, with additional consideration of the wind during take – off. For each configuration without wind, the TO distance was our limitation. Headwind greater than 10 ft/s limits the MTOW

with an assumed minimum climb rate. Since we expect windy conditions in Florida and Texas, we decided on a 216 in wingspan and an AR 15, which provides the greatest payload with the expected minimal wind.

### 3.2.2 Wing design

After second stage of optimization, we decided to use 216 in wingspan and 15 AR. We assumed TR between 0.5 – 0.6 to achieve optimal lift distribution along wingspan to reduce spar mass. The next step was the prediction of the achievable speed of the aircraft at the end of take - off roll, basing on tests of propulsion performance. Using previously mentioned MATLAB script for take - off analysis and measured propulsion performance, we predicted the take – off speed to be 17kts for MTOW = 32.17 lbs. We assumed 23.33 kts cruise speed, which is 1/3 higher than stall speed . Our experience with similar airframes from previous competitions suggests that the  $Re_{MIN}$  value should be no less than 225 000. These conditions, paired with the wingspan set to 216 in during optimization, led us to wing 16.3 inch root chord, 10 inch tip chord and 14.6 inch MAC. The wing was divided into multi - trapezoidal segments to obtain a half – elliptical outline, which was chosen to lower induced drag. A straight trailing edge minimizes 3D flow behind the wing [1]. This year's maximum part dimension restriction rule forced us to divide the wing into five sections, each of equal wingspan. Dihedral was applied to mid – and outer sections to improve the spiral stability (described in section 4.4). The ailerons were divided into three sections for better steering efficacy and redundancy. Fig. 6 is showing wing structure.

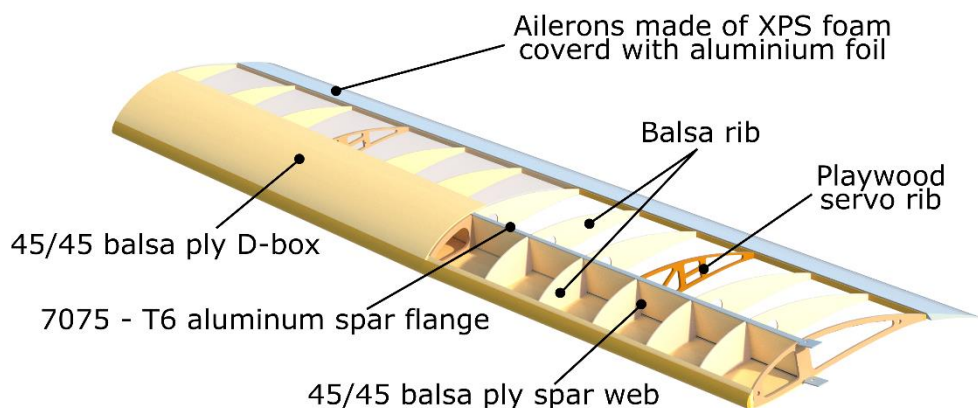


Fig. 6. Structure of a wing

### 3.2.3 Airfoil selection

As mentioned in 3.2.1, third stage of wing design was airfoil optimization. Although this year's aircraft is similar to our 2017 – 2019 designs, the airfoil LR315 from 2019 used in initial optimization was not perfectly suitable for the 2023 Regular class mission and our wing design. Therefore, the team modified LR315 and developed three new airfoils (MW 01.203, MW 01.202 and PP02) using Xoptfoil software. All three had a requirement of a minimum 13% thickness due to structural conditions. The center wing airfoil (MW 01.203) had a priority of high L/D ratio. The wingtip airfoil (PP02\_mod2) provides high  $CL_{MAX}$  to avoid wingtip stalls first. It differs significantly from MW 01.203 (mainly because of higher camber), so the third airfoil (MW 01.202) was designed to allow for a smooth transition between them. In the Fig. 7. airfoil characteristics are shown.

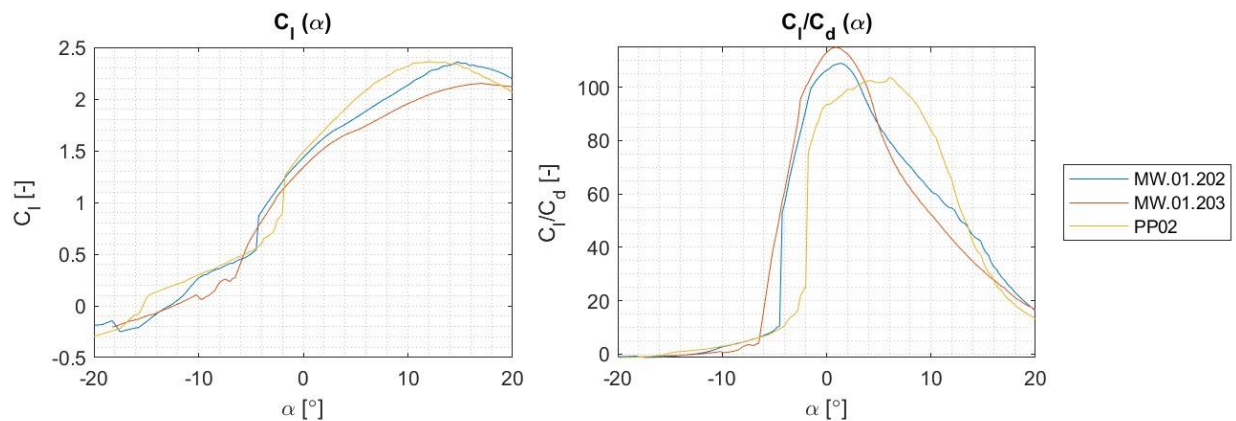


Fig. 7. Lift and drag coefficients plotted against attack angle

In the outer sections geometric twist is applied to achieve good stall characteristics. To ensure there will be no early flow separation on the wingtip, we plan to conduct wind tunnel testing of this section and, if necessary, install a vortex generator.

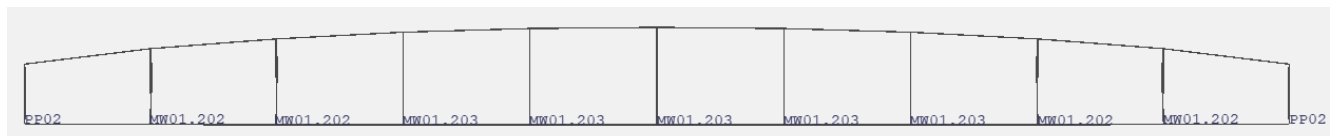
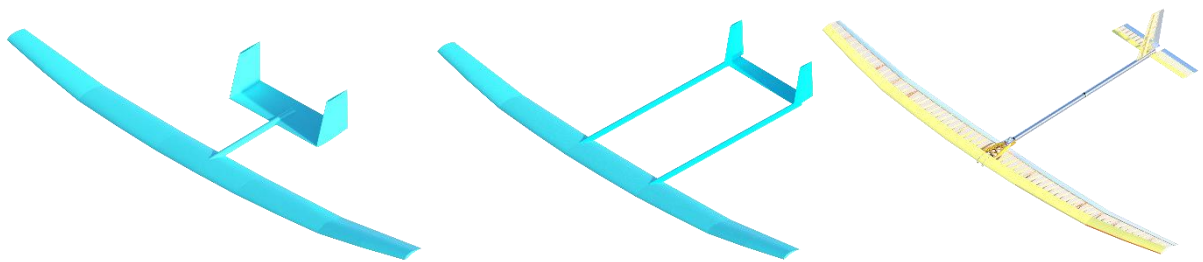


Fig. 8. Final wing planform with airfoils

### 3.2.4 Tail design

As we decided on 216 in wingspan, it was crucial to analyze the manufacturability of the tail boom before the second step of optimization. We realized that one piece tail boom, shorter than 48 in (due to the rules), would not provide simultaneously satisfying stability and performance. Longer tail boom requires splitting it into two or more sections and requires stiffer and stronger booms. Twin tail boom configuration would significantly complicate the structure of the wing/fuselage and also result in heavy tail configuration. We decided on half splitted, single boom empennage. The sizing factor for tail boom was deflection, not solely its ultimate strength. We assumed a maximum of 2 deg deflection at 75% of the maximum force within the flight envelope to prevent tail from swinging in windy conditions. That resulted in roller shaped boom with a constant 2.13 in. diameter. We designed lightweight CNC machined aluminum tail boom joints enabling disassembly of the boom into elements shorter than 48 in. To reduce mass, drag and simplify structure, we decided for T – tail empennage, with horizontal stabilizer mounted directly to the tail boom. Fig. 9 shows considered tail configuration. Elevator and vertical fin structure was designed according to the flight envelope.



*Fig. 9. Comparison of different configurations of the aircraft*

### 3.2.5 Fuselage, cargo bay and landing gear

The aircraft fuselage primarily intends to carry the payload, propulsion system and the propulsion system electronics for flight. In addition, the fuselage (with cargo bay) location relative to the wing was selected to lower CG and reduce possible damage in case of hard landing or crash. Moreover, we intended to accomplish simple construction of the fuselage. In result we designed this component as a separate part from the wing, with priority of time saving manufacturing and ease of maintenance.

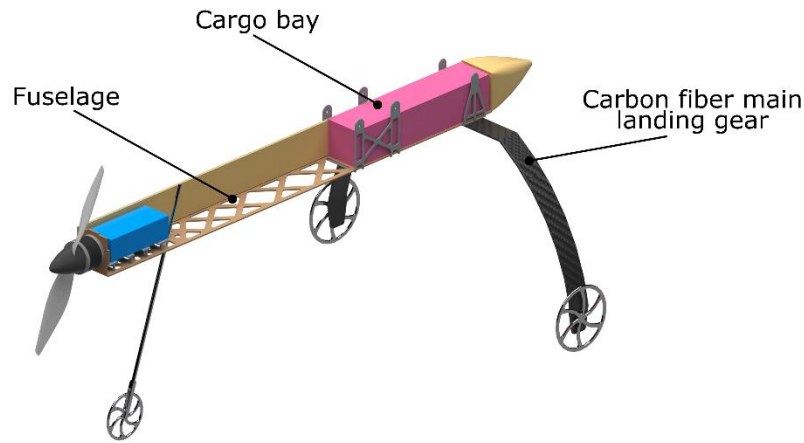


Fig. 10. Fuselage and its components

As for landing gear, we decided on three – point landing gear, with the front landing gear equipped with a shock absorber and commercially available carbon fiber landing gear to reduce mass and provide enough amortization to minimize the risk of damage to the aircraft during take – off and landing. Due to the long tail boom, we were obliged to choose high landing gear to prevent tail strike. Designed fuselage with marked cargo bay location I shown in the Fig. 10.

### 3.2.6 Mass and balance

We calculated the  $M_0$  of the aircraft by assigning proper density values for each part of the CAD model prepared in NX software. For manufactured parts, we multiplied the weight by factor 1.15 to include the mass of the glue weight. The empty weight was then used in scoring analysis to calculate the maximum possible payload. We also performed a balance analysis to ensure the proper location of CG. Mass and abalce table is shown below in Table 1.

Table 1. Mass of parts

No.	PART	MASS [Lb]	X [ft]	Moment of cg [lb - ft]
1	Wing	5.51	-0.03	-0.170
2	Horizontal tail	0.51	6.95	3.525
3	Vertical tail	0.44	7.17	3.160
4	Tail boom	2.09	3.01	6.312
5	Fuselage	1.43	-1.48	-2.122
6	Main gear	0.88	0.23	0.199
7	Front gear	0.55	-2.40	-1.323
8	Motor	0.79	-2.96	-2.347
9	Aileron servos	0.20	0.00	-0.001
10	Elevator servos	0.07	7.02	0.464
11	Rudder servo	0.03	7.18	0.237
12	Propeller	0.31	-3.06	-0.943
13	Main battery pack	1.65	-2.40	-3.968
14	Reciever	0.44	-0.10	-0.045
15	Servo electronic pack	0.26	-0.20	-0.053
16	ESC	0.26	-0.20	-0.053

17	Red arming plug	0.44	-0.82	-0.364
18	Ballast	0.32	-2.89	-0.924
I	M <sub>0</sub>	15.64	38.00 % MAC	
19	PAYLOAD	16.53	-0.09	-1.584
II	MTOW	32.17	33.00 % MAC	

### 3.2.7 Propulsion selection

Using previous years' experience and recognizing the maximum power as 750 W, we decided to use the Mn 605 320 kV motor for wind tunnel testing. After a preliminary propeller performance analysis, we decided to statically and dynamically test seven propellers from APC and Mejzlik companies, with diameters ranging from 21" to 30" and pitch from 10" to 12" (Fig. 12). Ultimately, we decided on the APC 21 x 12 propeller, which, despite having less static thrust (9,5 lbf), provided the greatest dynamic thrust (7,5 lbf) for a cruising speed of  $v = 23.33$  kts.

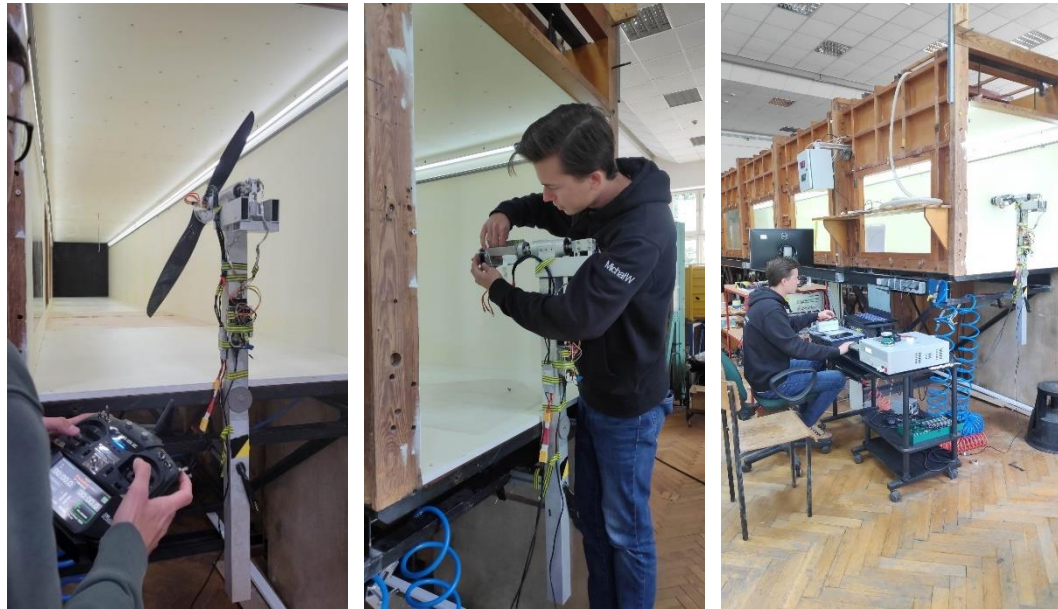


Fig. 11 Wind tunnel propulsion testing

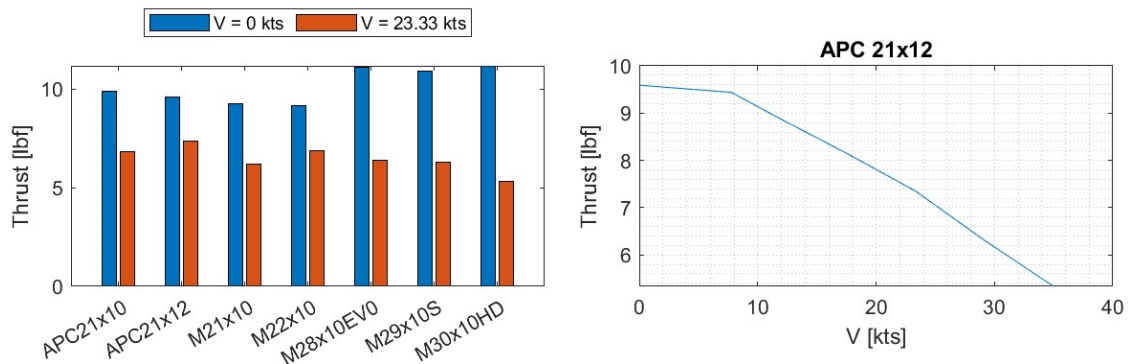


Fig. 12. Propeller performance comparison (left), selected propeller thrust characteristics (right)



### 3.2.8 Vehicle sizing and servo selection

The dimensioning of the aircraft was taken into account throughout the design process. Scoring analysis and optimization were used to dimension the plane. In addition, using experience from previous years, we were able to determine the size of the fuselage and the necessary undercarriage to withstand landing overloads. In order to ensure adequate control, the dimensions and hinge moments of the control surfaces were calculated with the XFLR5 program (using the VLM1 method) and further confirmed by calculations using basic flight mechanics methods. The analysis was performed for a speed of  $V_D = 35$  kts. Resulting hinge moments, assuming a control surface is a single panel, are presented in the Table 2. The aircraft uses 10 servos of the same type, of which 6 control the ailerons, 2 control the elevators, one controls rudder and one front landing gear. We decided to use the KST X08 Plus servo (torq. nom. 73.6 ozf in).

Table 2. Hinge moments on control surfaces.

Control surface	Span / height	Deflection	Reduction	Torque on servo (max) [oz · in]
Aileron	$b_l = 21.6 \text{ in}$	$+15^\circ, -25^\circ$	2:1	42.5
Rudder	$b_v = 17.7 \text{ in}$	$\pm 35^\circ$	4:3	40.6
Elevator	$h_h = 43.3 \text{ in}$	$+25^\circ, -25^\circ$	2:1	41.3

### 3.2.9 Structural analysis, load and material selection

We designed the aircraft according to CS – 23 requirements. Structural calculations were based on flight envelope calculated for the expected weather conditions. As mentioned before, we participate in SAE Aero Design East and West. In the middle of April in Texas we expect harsher weather conditions: stronger wind, higher temperature and lower air density. Basing on climate analysis and flight speed range, maximum load factor was assumed to be +4 and -1. Design cruise speed was 23.33 kts ( $V_C$ ). Due to expected strong wind and gusts we assumed the diving speed ( $V_D$ ) as 38.9 kts. We decided to use 1.5 safety factor for all the aluminum parts of the wing spar. The FOS of the balsa structure was determined as 2.5, basing on the [3] due to wide range of balsa wood properties.



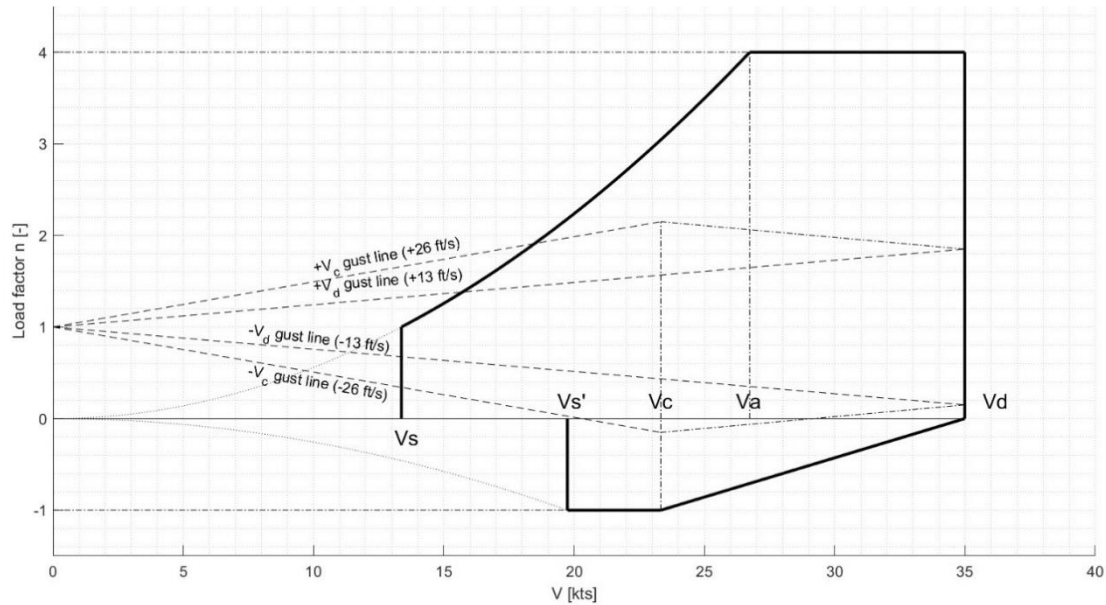


Fig. 13. Flight envelope

According to the measurements made with PixHawk during flight tests in previous years, the landing shock is approximately -2.5 g. For other parts of the aircraft, we used a safety factor of 1.25. The strength – to – weight ratio was an important criteria in material selection, as well as cost and availability of materials. Basing on flight envelope, we calculated loads in spar and D – box. We selected aluminum alloy 7075 – T6 for the spar flanges, because of high yield strength, low density and easy manufacturing. Spar flanges geometry was calculated basing on lift distribution. D – boxes were made of 2 – layer balsa plywood (0.06 in on the center wing, 0.03 in at the wing tips) with 45/45 grains orientation. To reduce the mass of spar wall and prevent from buckling, we made a sandwich structure of 2 – layer balsa with PVC foam (Herex) between them. Higher loaded ribs were made out of plywood. The other ribs were made of balsa to reduce the weight of the wing. To provide good airfoil representation the ribs were laser – cut or milled on a CNC machine. Wing, fuselage and empennage is covered using OraLight foil to achieve smooth surface and reduce mass (wing structure is shown in Fig. 6).

As mentioned in 3.2.4 section, the tail boom deflection was the dimensioning criterion. To meet this requirements tail boom was made of two layers of steel foil (0.002 in) and balsa wood (0.08 in) between them. This year, because of the requirements of the regulations, the tail boom of our aircraft is made of two parts. In order to assemble

and dismantle the aircraft efficiently, we designed the joints CNC machined from 7075 aluminum alloy. Spar of horizontal and vertical stabilizer were manufactured from lime wood which has higher strength than conifers wood.

### 3.2.10 Spar wall structure and testing

A detailed theoretical analysis of the strength of the wing wall under shear force allowed to reduce spar mass by redesigning the structure. Material tests were carried out in a double articulated frame, which operates in pure shear under the transmission of forces through its perimeter. Spread of ultimate strength was 16,9% what is acceptable comparing to 15,4% in [2]. Understanding risk of error during manufacturing, we decided for 2.5 safety factor for calculations of spar wall balsa structure.

### 3.2.11 Wing static test

To verify our calculations and the reliability of the structure, we are going to conduct static tests of the wing. We will perform the test for 100% of the maximum bending loads in flight, achieved at point A of the flight envelope. Fig. 14 shows the bending moment distribution along the wing span at point A of the flight envelope.

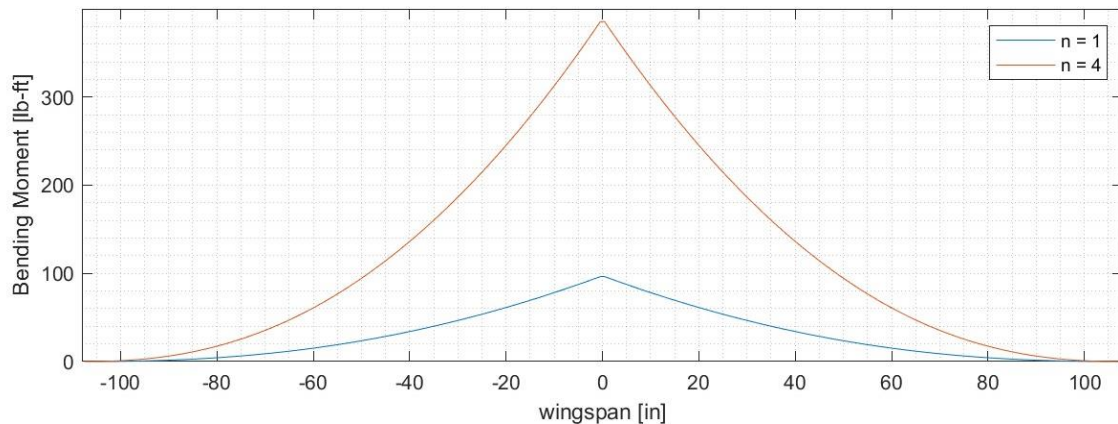


Fig. 14. Bending moment

The wing will be progressively loaded with weights distributed along the wing span during the test. We will measure the deflection of the wing tip for an increasing load and compare it with the calculated deflection. We will also observe whether there is any damage to the wing structure. We planned end of the wing's building is early February. At that time, we intend to conduct static tests; for this reason, we cannot yet include photos of the tests and their results.

### 3.3 Final structure design

#### 3.3.1 Assembly

In order to allow transport in a container and fulfill the requirements of the regulations, the aircraft is divided into 10 main parts. The connections between the parts are designed to make assembling and disassembling the aircraft comfortable and quick. As a result, preparing the aircraft for flight takes little time and does not create additional difficulties.

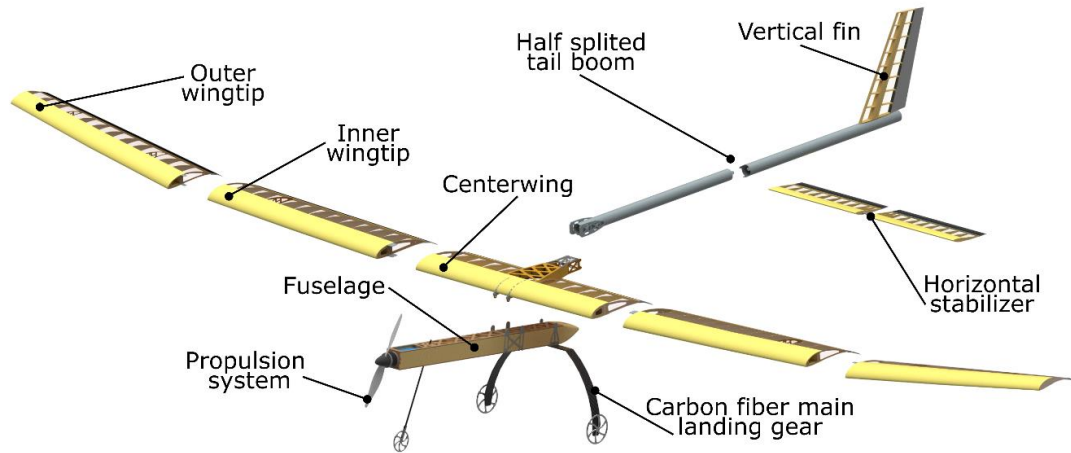


Fig. 15. Exploded view

#### 3.3.2 Design features

The most challenging part of our aircraft, both in design and manufacturing, is the five part wing, which parts are connected to each other with only one bolt each. This allows the aircraft to be quickly assembled and ready for flight on the runway.

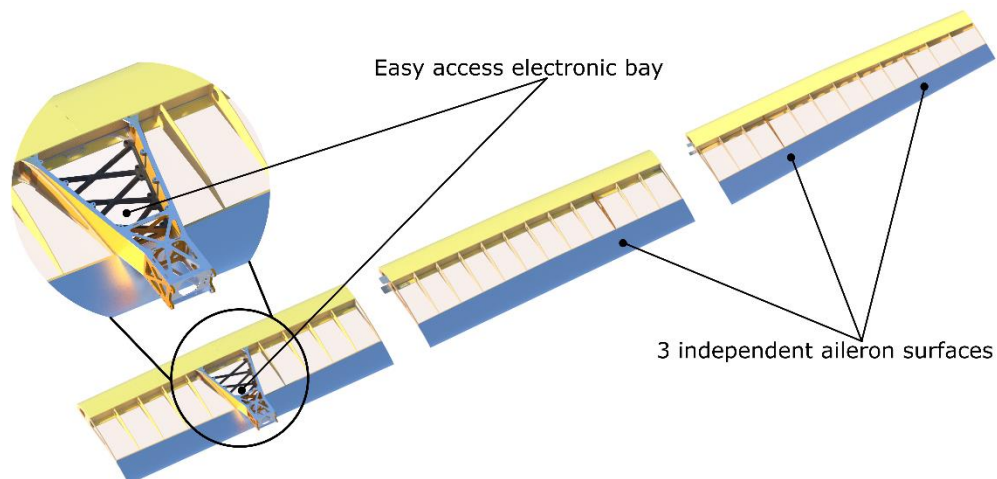
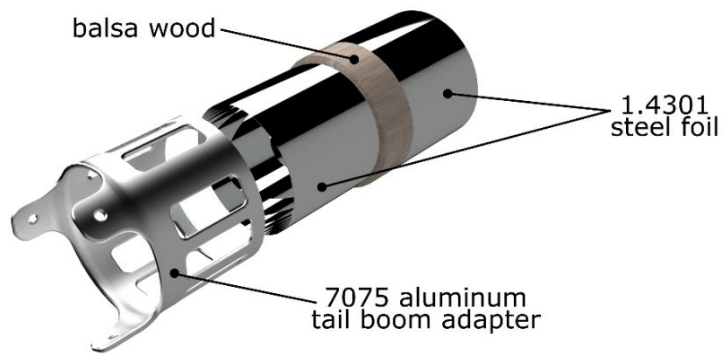


Fig. 16. Wing and electronic bay

In the center wing is the easily accessible large electronics bay (with receivers, telemetry devices and auxiliary battery pack). Six independent ailerons provide high redundancy and improves aircraft performance. As described before tail boom of our aircraft consists of two parts, which are connected to each other with lightweight CNC milled joints (0.057lbs each).



*Fig. 17. Tail boom exploded view with adapter*



*Fig. 18. Adapters for the tail boom segments (joined)*

## 4. Performance Analysis

### 4.1 General

The performance analysis was carried out to verify the accuracy of the initial design assumptions and to anticipate and prevent potential risks during the flight. As a result, we were able to provide a payload prediction.

### 4.2 Weather conditions

We analyzed weather conditions to predict air density and collected information on wind direction and speed based on climate data. We based our calculations on data presented in table below.

*Table 3. Weather conditions*

Elevation	Avg. high temp.	Pressure	Avg. wind speed (10 AM - 4 PM)	Max. gust wind	Wind direction	Air density
194 feet	77° F	30.09" Hg	11.6 mph	15.2 mph	28% east, 27% north	0.00225 slugs/ft <sup>3</sup>

### 4.3 Take off and climb analysis

To analyse TO and climb we developed MATLAB application to estimate aircrafts performance. Limited power and take off distance require to precisely simulate take – off ground roll including rotation phase to not exceed the take – off distance and each appropriate speed before the transition phase. For accurate simulation, each phase was simulated by determining the forces and moments acting on the on the aircraft.

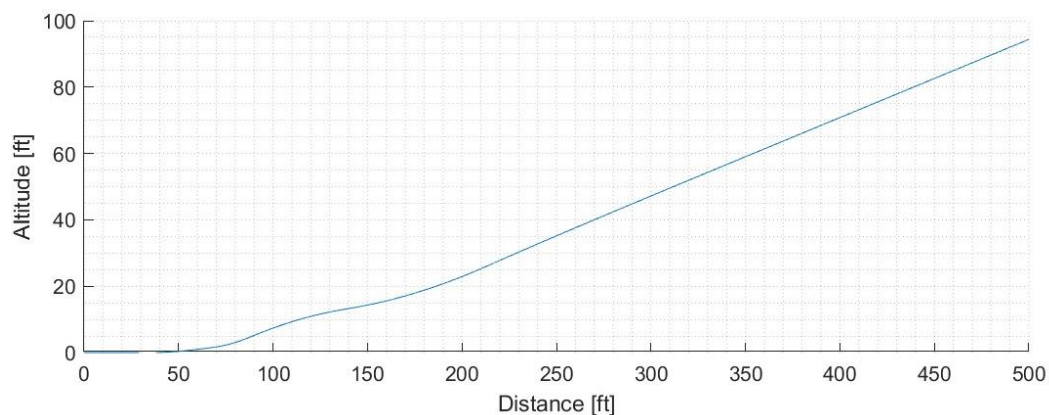


*Fig. 19. Take - off analysis*

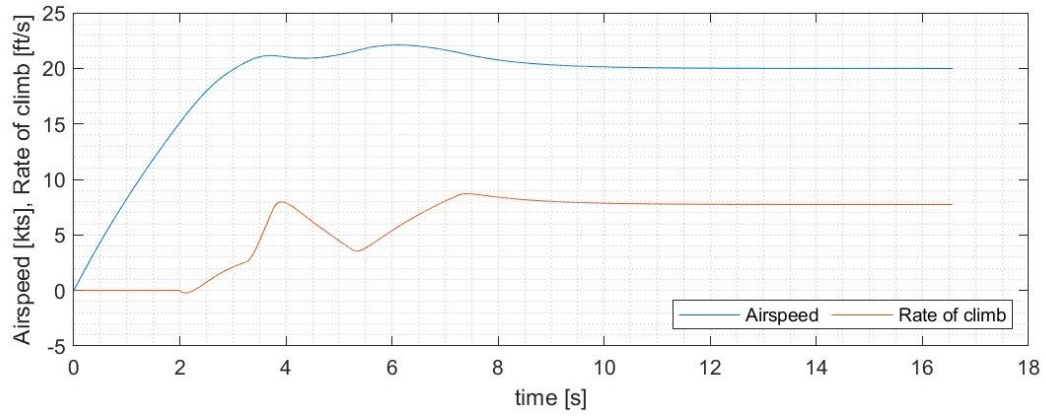


Fig. 20. Take - off analysis

A climb rate analysis was made to ensure that the aircraft can reach safe altitudes margin over obstacles to perform a turn. According to our assumption, the climb rate should exceed 7 ft/s .

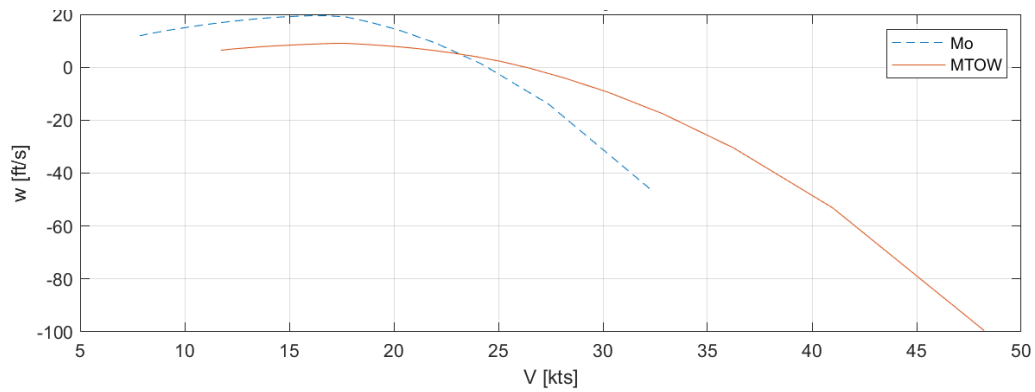


Fig. 21. Climb rate analysis

#### 4.4 Stability and control

Stability was analyzed according to the CS – 23 regulations using Panukl and SDSA software developed at our faculty. First step was to calculate static stability to size up empennage and reach 20% stability margin for TO weight for speed range from 17.5 kts to 31.1 kts for CG located at 30% of MAC. This ensures that small error in balancing the aircraft before flight would not result in serious stability problems.

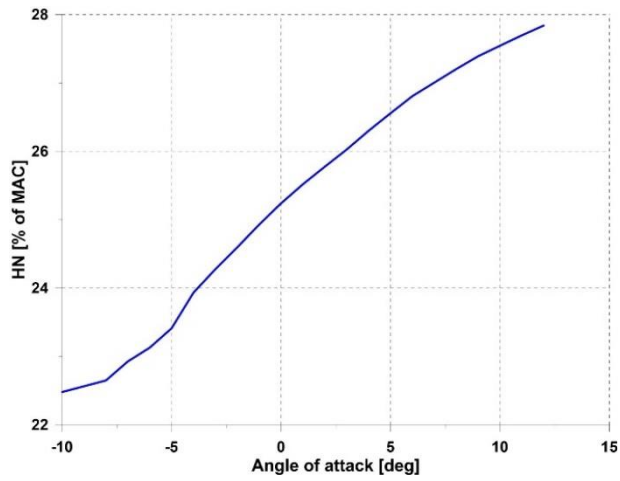


Fig. 22. Static margin vs. angle of attack

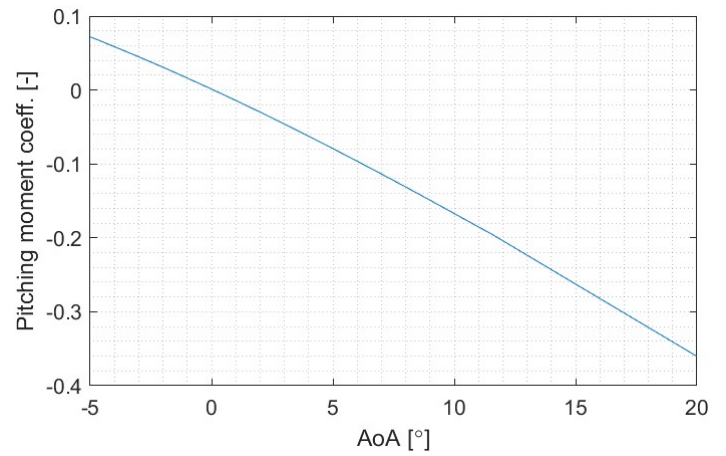


Fig. 23. Pitching moment coefficient vs. angle of attack

Second step was dynamic stability analysis using moments of inertia obtained from mass and balance analysis. We ensured that any combined lateral-directional oscillations will be damped to at least 1/10 in 7 cycles. Additionally polyhedral wing significantly improved spiral stability. Final results were compared using AVL and XFLR5 software with no significant differences. Furthermore, we conducted roll analysis to meet the CS – 23 requirements. Results showed that ailerons on 3/5 of the wingspan with deflection (+15°/-25°) provide enough angular roll velocity. Below is shown characteristics of dutch roll and spiral mode time against the background of MIL – F8785C specification.

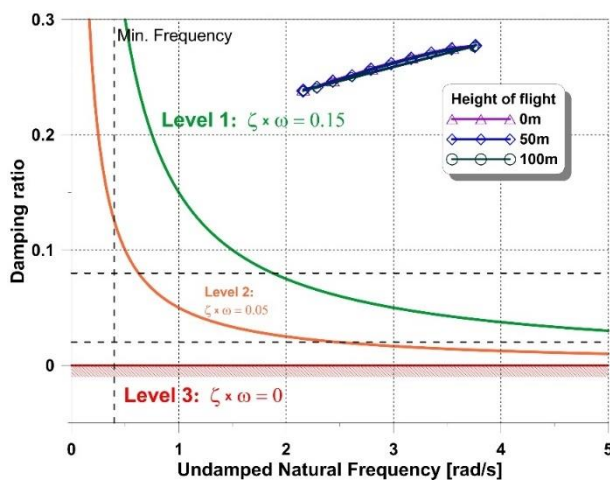


Fig. 24. Dutch roll characteristics against the background of MIL - F8785C specification

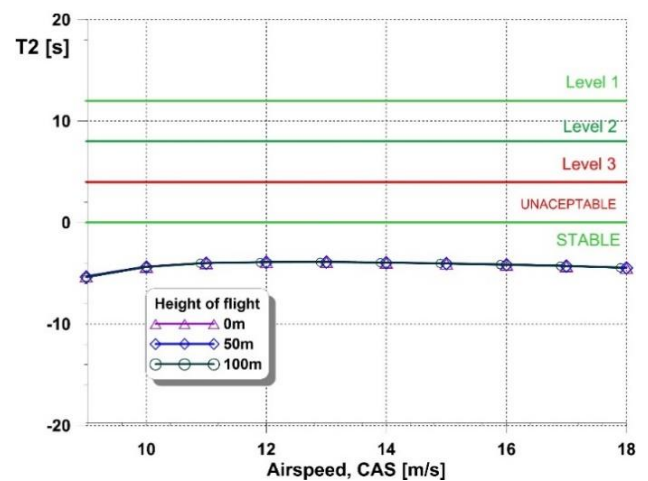


Fig. 25. Spiral mode time to double against the background of MIL - F8785C specification



## 4.5 Turn Radius Analysis

Considering the equations of rotational motion we calculated the turn radius in relation to the bank angle. The chart below shows that at the speed of 24 kts and the bank angle of 10 degrees that the aircraft performs a turn with the radius of 300 ft. This ensures the flight within available space.

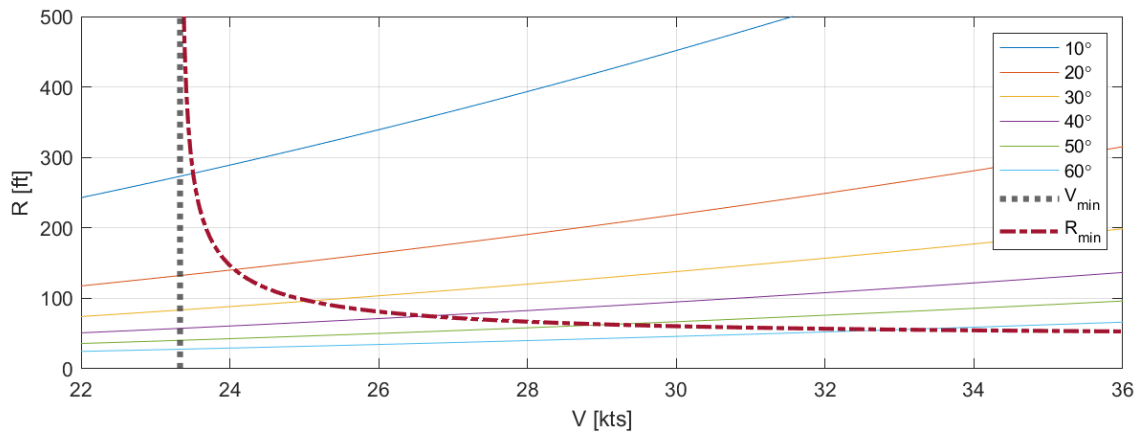


Fig. 26. Turn radius analysis

## 4.6 Polar curve and landing distance

A polar curve was made for the landing analysis (Fig. 27). The best descent angle ( $2.38^\circ$ ) was obtained for an aircraft with a full load (MTOW = 32.17 lbs ) and a speed of 18 kts at the start of the descent. Using this analysis and assuming an altitude of 34 ft at the beginning of the descent, we prepared a distance analysis for 4 phases: descent, flare, touchdown, and after – landing roll. The results (Fig. 28) allowed us to determine the 180 ft reserve needed to land at the 400 ft required by the competition rules.

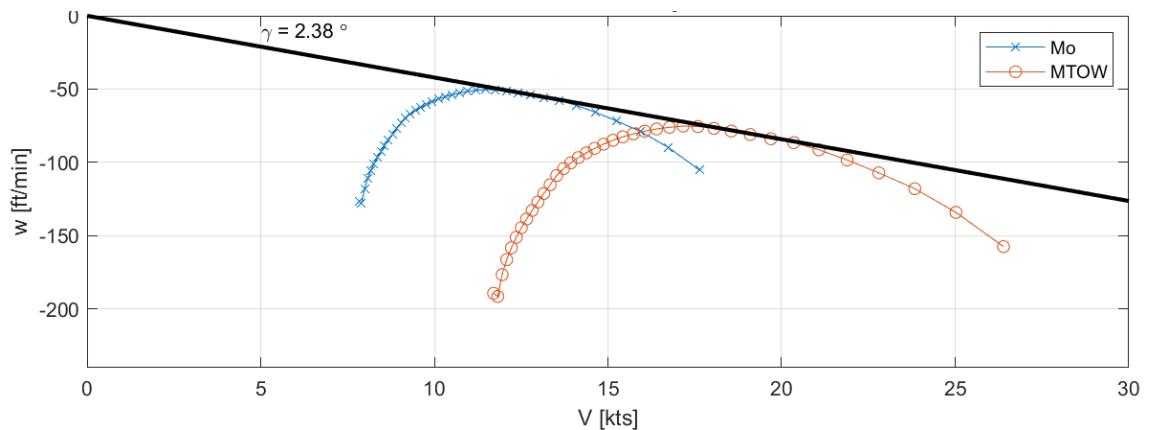


Fig. 27. Polar curve analysis



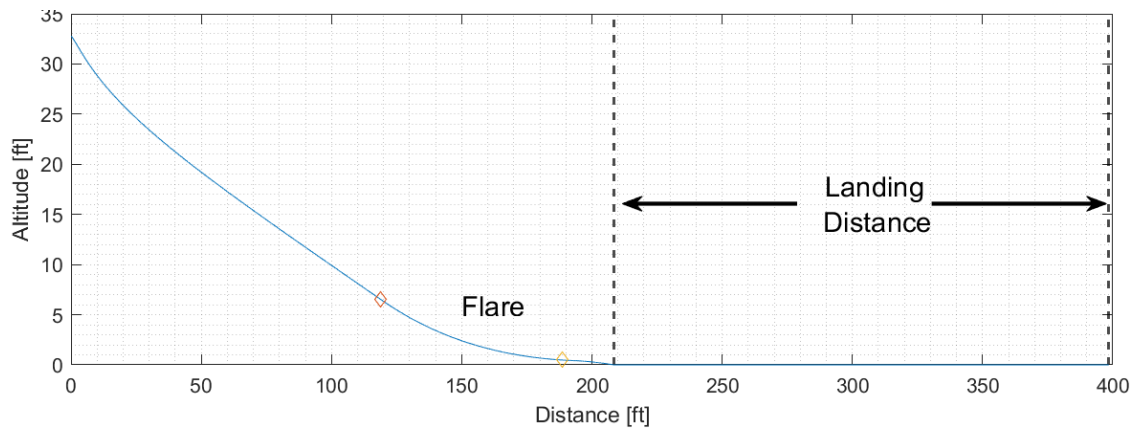


Fig. 28. Landing analysis

#### 4.7 Payload prediction and lifting performance

The load prediction curve (Appendix 1) was created from the performance analysis with the following assumptions:

- the calculated take - off distance should not exceed 100 ft,
- the rate of climb should not be less than 400 ft/min,
- radius of the turn not greater than 300 ft,
- landing distance not greater than 400 ft,
- wind is not taken into account.

## 5. Manufacturing

For the construction of the plane, we used mainly balsa wood, plywood and 7075 T6 aluminium which have the best strength – to – weight ratio. To assemble structure and provide proper positioning during gluing process we made acrylic retainers. To achieve expected performance it was necessary to precisely represent designed geometry. This year we implemented new precise spar positioning device (Fig. 33) to achieve designed dihedral and interchangeability between two builded airplanes. Positioning error of 0.02 in along wingspan could result in 0.8 degrees dihedral change.



*Fig. 29. In - house manufacturing of servo - ribs*

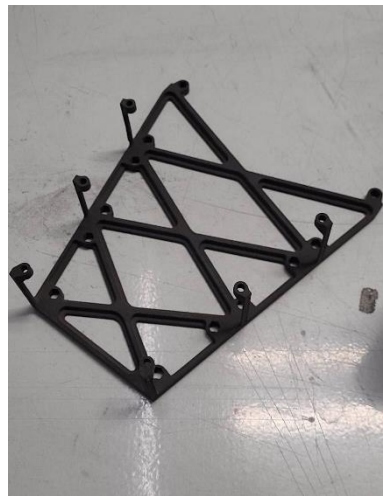


*Fig. 30. 3D SLS printed element of center wing - electric bay*



*Fig. 31. 3D SLS printed element of tail boom*

All major parts such as wings, spar wall, spar flanges, ribs, bars, retainers were CNC machined or cut on laser. The precision of manufacturing of these components directly affects the aerodynamics and structure strength. Most parts we made using our CNC router, while the production of more complicated parts was outsourced to professional companies. Thanks to our new sponsor we were able to implement SLS 3D printing into our design. This allowed us to design lightweight tail boom reinforcement to prevent from buckling near mount to the centerwing – the highest stressed part (Fig. 31). The D – box covers, spar walls, and tail boom were bonded under vacuum on positive form representing wing surface (Fig 32). We were able to use less glue without worrying that the joint would not be strong enough. By reducing the amount of glue, we also reduced the weight of the entire airplane. It was important to verify the mass of the design during the manufacturing process.

Upper D-box cover was glued on acrylic retainer (Fig.34). To achieve designed geometrical twist bottom D-box cover was glued on wing structure which was placed in CNC milled negative form.

One entire five-part wing require over 170 parts manufactured on CNC or laser cut. To organise work we developed part naming and numerating system and prepared manufactuirng manulas with checklists to reduce risk of human error.

In late November we performed glue strenght test and selected proper gluing method for each type of materials. We used wood glue, epoxy resin glue with and 3M DP 490 glue for bonding metal to metal and metal to wood. Knowing each glue properties, especially 3M glue we understand the need for protection the aircraft against heating on ground.

The tail boom was made on a cylindrical rod on which successive layers of steel foil and balsa were glued. After the balsa was bonded to the inner layer of steel foil, the adapters were installed and then the outer layer of foil was applied. Development of this technology allowed us to manufacture rigid boom that is also much lighter than a traditional truss structure.



*Fig. 32. D - box covers during vacuum gluing*



*Fig. 33. Spare flange positioning device, acrylic retainer*



*Fig. 34. D - box covers during gluing to the wing structure*

## 6. Conclusions

---

Along with new challenges come new opportunities to prepare for new competitions. This year, we were finally able to put the pandemic past behind us and focus on designing and building even better airplanes. One of the most significant challenges this year was undoubtedly to prepare for both editions of the competition, making the preparation time much shorter.

In addition, due to starting with two aircraft for the event, we had to adapt the work to the limited space. These challenges taught us vital skills such as planning, management, optimization and production technologies. In addition, the analysis carried out both theoretically and during experiments allowed us to set the parameters as accurately as possible, allowing us to fight for the top places in this year's competition.

## Appendices

---

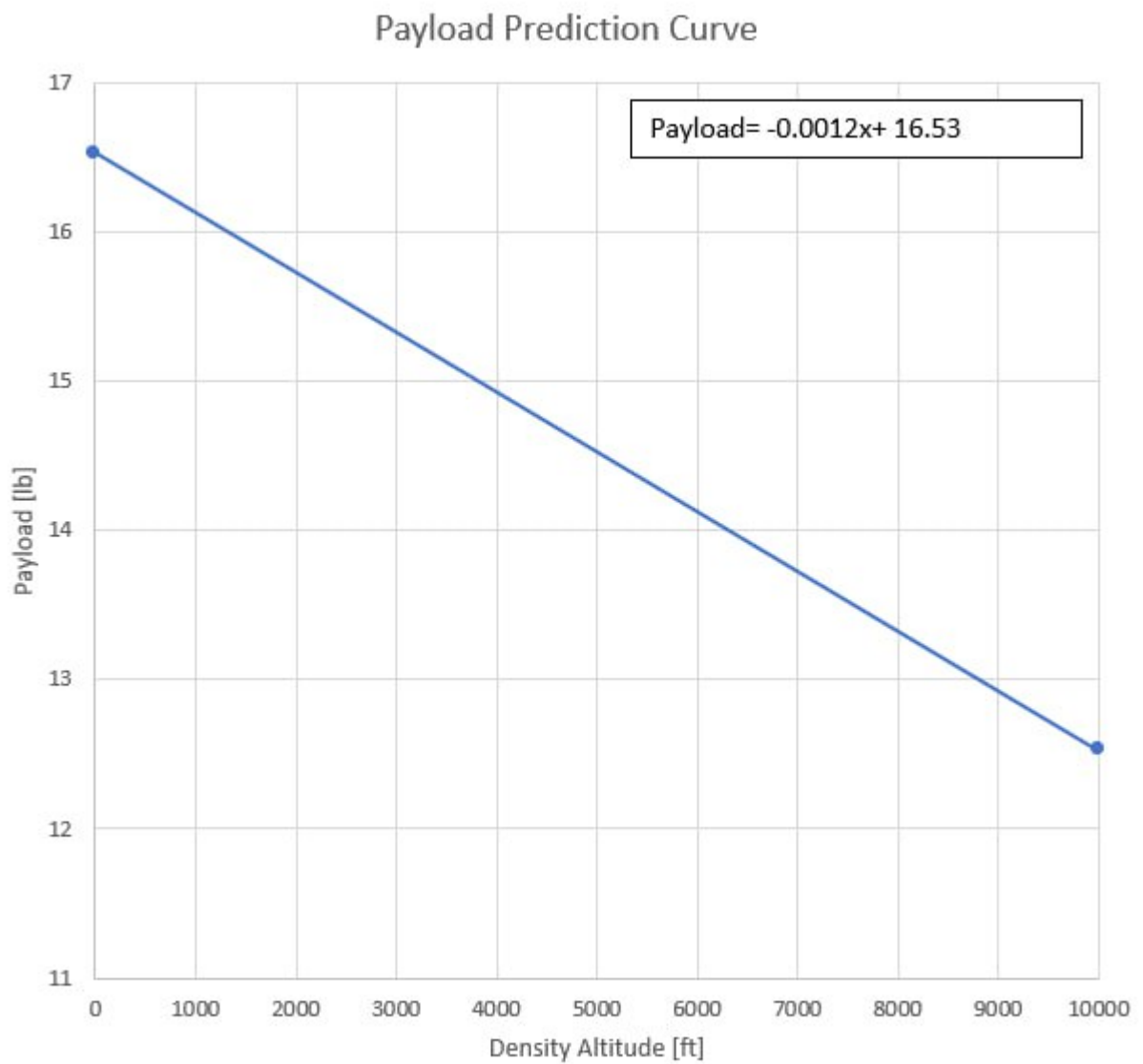
1. Technical Data Sheet-Payload Prediction Curve Team 035
2. 2D Drawing Team 035

# Payload prediction curve

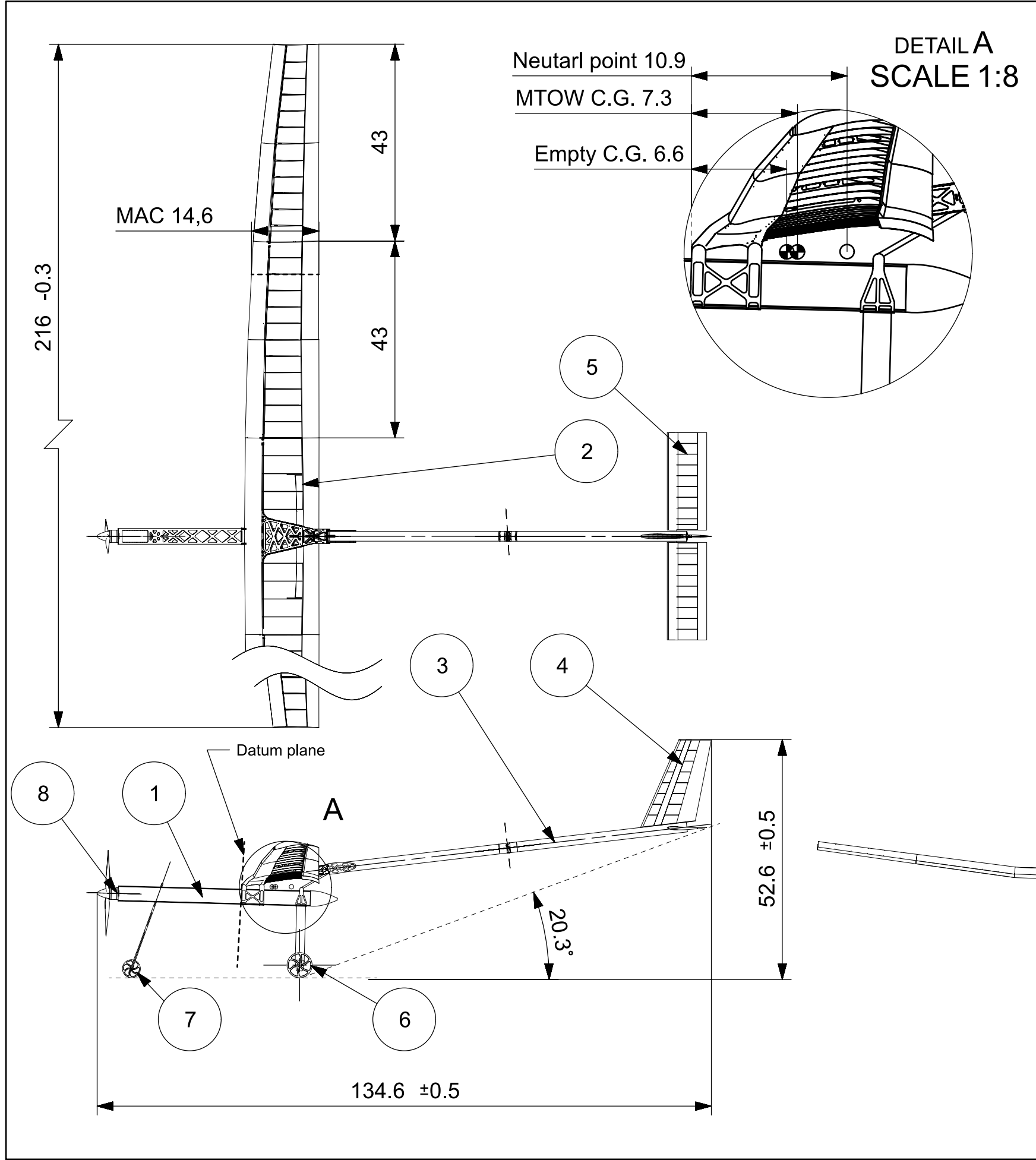
Team name: WUT Regular

Warsaw University of Technology

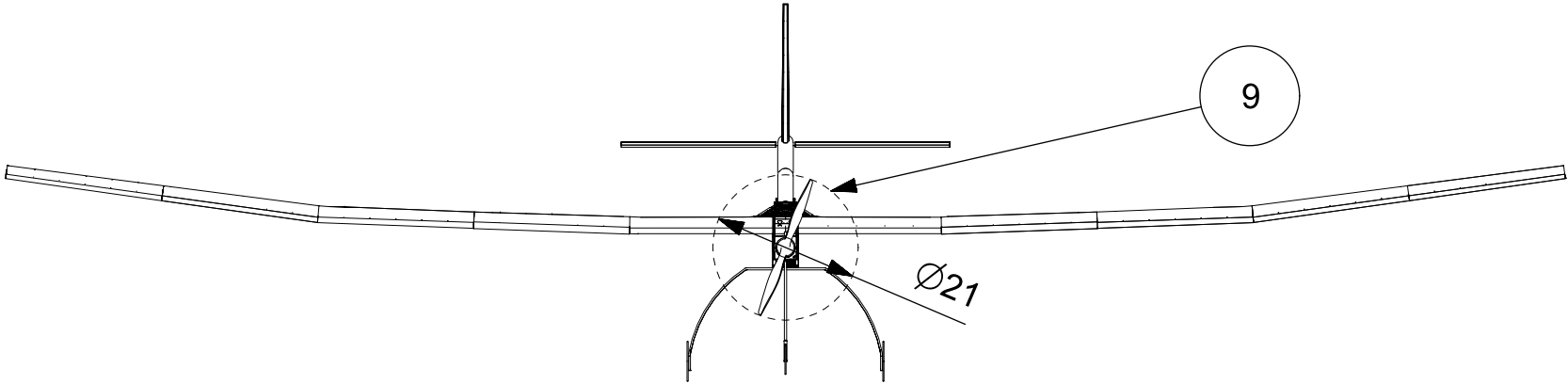
Team number: 035



Explanation can be found in section 4.7 of the Design Report.



Mass and Balance					Part list		
No.	Part	Mass [lbs]	Arm [in.]	Moment [in.*lbs]	No.	Part	Specification
1.	Wing	3.44	6.77	23.29	1	Fuselage	
2.	Tailboom	2.09	43.31	90.70	2	Wing	Span: 216in. Area: 3162sq.in. Aspect ratio: 15
3.	Fuselage	1.43	-10.63	-15.23	3	Tailboom	Split in two parts
4.	Battery 5000mAh	1.65	-21.65	-35.80	4	Vertical stabilizator	Height: 17.7in. Area: 174sq.in. Aspect ratio: 1.8
5.	Electronic eq.	0.44	5.91	2.60	5	Horizotna stabilizator	Span: 45in. Area: 405sq. in. Aspect ratio: 5
6.	Battery 1000mAh	0.26	4.72	1.25	6	Main landing gear	Two wheels 4.7in. diameter
7.	Safety plug	0.44	-2.76	-1.22	7	Forward landing gear	Single wheel 3.9in. diameter
8.	Landing gear servo	0.3	-21.65	-0.72	8	Motor and ESC	Motor: T-Motor NM605 320KV ESC: APD 100A F3 max current100A
9.	ESC	0.26	-24.41	-6.46	9	Propeller	APC 21x12
10.	Motor	0.79	-28.35	-22.50	Servo spec		
11.	Propeller	0.31	-29.53	-9.11			
12.	Main landing gear	0.88	9.84	8.68	6x aileron 2x horizotnal stabilizator 1x landing gear 1x rudder		
13.	Forward landing gear	0.55	-21.65	-11.93			
14.	Horizotnal stabilizator	0.51	90.55	45.92	KST Micro X08 Plus Wing momnet: 0.38 ft/lbs		
15.	Vertical stabilizator	0.44	93.15	41.07			
16.	Balast	0.32	-27.56	-8.81			
Empty C.G.		13.87	38% of MAC				
17.	Cargo	18.30	6.07	6.61			
MTOW C.G.		32.17	33% of MAC				



Team number 035	WUT Regular	Warsaw University of Technology
01/29/2023	Design M. Włodarczyk	Scale 1:25